Journal of Applied Sciences

ISSN 1812-5654

science alert

ANSInet
an open access publisher
http://ansinet.com

Journal of Applied Sciences 10 (23): 3032-3041, 2010
ISSN 1812-5654

Automated Fault Location in a Power System with Distributed Generations using Radial basis Function Neural Networks

[1]H. Zayandehroodi, [1]A. Mohamed, [1]H. Shareef and [2]M. Mohammadjafari
[1]Department of Electrical, Electronic and Systems Engineering, University Kebangsaan Malaysia, Malaysia
[2]Department of Engineering, Islamic Azad University of Kerman, Kerman, 7635131167, Iran

Abstract: High penetration of Distributed Generation (DG) units will have unfavorable impacts on the traditional fault location methods because the distribution system is no longer radial in nature and is not supplied by a single main power source. This study presents an automated fault location method using Radial Basis Function Neural Network (RBFNN) for a distribution system with DG units. In the proposed method, the fault type is determined first by normalizing the fault currents of the main source. Then to determine the fault location, two RBFNNs have been developed for various fault types. The first RBFNN is used for detraining fault distance from each source and the second RBFNN is used for identifying the exact faulty line. Several case studies have been used to verify the accuracy of the method. Furthermore, the results of RBFNN and the conventional Multi Layer Perception Neural Network (MLPNN) are also compared. The results showed that the proposed method can accurately determine the location of faults in a distribution system with several DG units.

Key words: Fault location, Distributed Generation (DG), power system, Radial Basis Function Neural Network (RBFNN), perception neural network (MLPNN)

INTRODUCTION

With increasing reliance on electricity, customers demand reliable power supply with reduced outage time and operating costs. When a fault occurs in a distribution network, it is important to quickly locate the fault by identifying either a faulty bus or a faulty line section in the network. Without locating the faulty section, no attempt can be made to remove the faults and restore the power supply. Fault location in electric power distribution systems still presents many challenges due to its varied topological and operational characteristics. The traditional methods used for locating faults in a distribution network include visual inspection, traveling wave method and the use of utility outage management system to identify circuit outages. However, these traditional fault location methods are unable to locate faults quickly. To locate fault location, voltage and current values are generally measured using intelligent electronic devices installed at substations. Although, these data loggers can capture the fault events precisely, they are not equipped with fault diagnostic algorithms, which can quickly identify fault location. To solve this problem, an automated fault location using intelligent data interpretation system is required (Mohamed and Mazumder, 1999).

Several artificial intelligence techniques have been developed for automated fault location in distribution systems (Jun *et al*., 1997; Wen and Chang, 1998; Mohamed and Mazumder, 1999; Chien *et al*., 2002; Fei and Ying, 2003; Brahma, 2005; Senger *et al*., 2005; Borghetti *et al*., 2006). The intelligent based fault location methods locate faults by calculating the fault distances, identifying the faulted phases and locating the faulty protective devices. These methods, however, do not consider distribution networks with Distributed Generation (DG). From a technical viewpoint, the presence of distributed generators in a distribution network would result in some conflicts in the operation of the present network because distribution network configuration is no longer radial in structure. The conventional fault location scheme is suitable for locating faults in a system with a single source radial supply line or with multi-source open loop operation. With the increasing penetration of DG, the distribution system becomes a multi source system and the system configuration is not radial. In such network, determining the exact location of faults is becoming complicated, as faults are fed by multi-sources. Hence, the existence of DGs in a distribution network poses a difficulty in locating faults in the network.

Corresponding Author: Hadi Zayandehroodi, Department of Electrical, Electronic and Systems Engineering, University Kebangsaan Malaysia, Malaysia Tel: 0060173141329

Recently, fault location methods have been developed by considering DGs in a distribution network (Ma *et al*., 2008). A fault location algorithm for a distribution system with DGs has been developed by using current measurements (Guo-Fang and Yu-Ping, 2008a, b). In this method, after a faulted segment is located, islands are formed involving groups of DGs and a load shedding scheme is implemented to match the loads with the DGs generating capability in the island. This method requires a mechanism to reconnect the disconnected loads after faults are removed. A method for finding the exact location of faults in a network with DG has been developed based on software procedures which require a telecommunication control system (Conti and Nicotra, 2009). Another fault location method is based on the estimates of the fault impedance by measuring current and voltage at a substation (El-Fouly and Abbey, 2009). In this method, the fault location performance is inaccurate when a DG is located upstream of the fault section where the impact is more severe for synchronous machine based DG. An asymmetric fault location method using a communication system has been developed by identifying the direction of an asymmetrical fault based on negative sequence current scalar product (Du *et al*., 2009). Here, an asymmetrical fault line searching and locating scheme is implemented by combining the fault direction distinguishing method with its communication system. A more recent fault location method for a distribution network with DGs considers the application of Multi Layer Perceptron Neural Network (MLPNN) (Rezaei and Haghifam, 2008; Javadian *et al*., 2009a, b). However, considering the structure and training algorithm of the MLPNN, the speed of this method is not suitable for fast and accurate fault location.

The aim of the research is to develop an accurate and automated fault location method for a distribution network with distributed generators by identifying the faulty line. This study presents an automated fault location scheme for a distribution network with DGs using the Radial Basis Function Neural Network (RBFNN). RBFNN is considered to be a better neural network model for solving engineering problems. The proposed scheme determines the fault type by normalizing the fault current of the main source whereas the location of faults is determined by using two RBFNNs. The first RBFNN determines the fault distance from each DG and the main source while the second RBFNN identifies the exact faulty line.

RBF NEURAL NETWORK

The RBF Neural Network (RBFNN) is a feed-forward neural network having three layers, namely, an input layer, hidden layer and output layer. The input layer feeds the values to each of the neurons in the hidden layer. The hidden layer consists of neurons with radial basis activation functions and an output layer consists of neurons with linear activation function. A generic architecture of an RBFNN with k input and m hidden neurons is shown in Fig. 1.

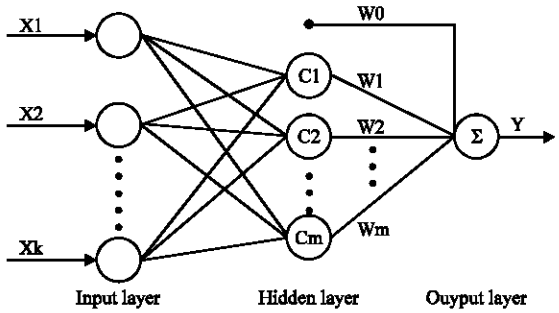

Fig. 1: A generic architecture of the RBFNN

In the training of the RBFNN, the following computations are considered. When the network receives a k dimensional input vector X, the network computes a scalar value using:

$$Y = f(X) = w_O + \sum_{i=1}^{m} w_i \varphi(D_i) \quad (1)$$

where, w_0 is the bias, w_i is the weight parameter, m is the number of nodes in the hidden layer and (D_i) is the RBF.

In this study, the Gaussian function is used as the RBF and it is given by:

$$\phi(D_i) = \exp\left(\frac{-D_i^2}{\sigma^2}\right) \quad (2)$$

where, σ is the radius of the cluster represented by the center node, D_i is the distance between the input vector X and all the data centers.

The Euclidean norm is normally used to calculate the distance, D_i which is given as:

$$D_i = \sqrt{\sum_{j=1}^{k} \left(X_j - C_{ji}\right)^2} \quad (3)$$

where, C is a cluster center for any of the given nodes in the hidden layer (Yu *et al*., 2008).

The implementation procedures in the training of the RBFNN are presented as follows:

Step 1: Obtain input data and target data from the simulation

Step 2: Assemble and preprocess the training data for the RBFNN

Step 3: Create the network object and train the network until condition of network setting parameters are reached

Step 4: Test and conduct regression analysis

Step 5: Stored the trained network. Steps (1-5) are offline processes

Step 6: Preprocess the new input before they are subjected to the trained network to obtain required data

IMPLEMENTATION OF FAULT LOCATION IN A DISTRIBUTION NETWORK WITH DG USING RBFNN

An important consideration in the protection of distribution networks is the determination of the type and location of faults occurring in its protection zone. In this work, normalized fault current of the main source is used for determining the various types of faults. On the other hand, the fault location in a distribution system with DGs has been developed using RBFNN.

Identification of fault type: At normal operating conditions, the sum of current contribution from all sources is equal to the total load current. When a fault occurs at any point, fault current will be significantly larger than the total load current. Thus, a comparison between the total currents of generators and loads can be used for the detection of fault conditions. To identify the various fault types, the 3 phase currents of the main source from the feeding substation are used. The three phase output fault currents at the main source or the feeding substation are normalized using:

$$I_{normal} = \frac{I}{I_{max}} \quad (4)$$

where, I is the fault current and Imax is the maximum fault currents for each type of fault.

Based on the normalized three phase fault currents and rounding the obtained values to the nearest one, the types of faults can be classified as shown in Table 1 (Gers and Holmes, 2005). From the Table, 1, -1 and 0, indicate that a fault occurs in the phase, a fault occurs in the phase but the short circuit current is in the opposite direction and no fault, respectively. The symbols Ag, Bg and Cg indicate the single phase to ground faults for phase A, B and C, respectively while symbols AB, AC and BC indicate the phase to phase faults for the respective phases. Consequently, symbols ABg, ACg and BCg indicate 2 phase to ground faults for the respective phases.

Table 1: Fault type classification data

Fault type		I_a	I_b	I_c
1-phase to ground	Ag	1	0	0
	Bg	0	1	0
	Cg	0	0	1
phase to phase	AB	1	-1	0
	AC	1	0	-1
	BC	0	1	-1
2-phase to ground	ABg	1	1	0
	ACg	1	0	1
	BCg	0	1	1
3 -phase	ABC	1	1	1

Determination of fault location: After identifying the fault type, its location should be determined. In this study, two stages of RBFNN have been developed in which the first RBFNN is for determinings fault distances from the main source and the two DG units (RBFNN1, 3, 5, 7) and the second RBFNN (RBFNN 2, 4, 6, 8) is for determining the faulty line for the respective fault types. Figure 2 shows the procedures in determining the fault location. From the figure, for each fault type first, the 3 phase currents of main source and all the DGs are used as inputs to the first RBFNN. The outputs of the first RBFNN which are the distances of fault from the main source and the DGs are then used as inputs to the second RBFNN. Hence, the output of the second RBFNN is the exact faulty line.

SIMULATION RESULTS AND DISCUSSION

To verify the performance and accuracy of the proposed fault location method using the RBFNN, the 22 bus, 20 kV distribution network with 2 DG units is selected as the test system as shown in Fig. 3. The system consists of a 4.5 MVA diesel generator as DG1 connected to bus 4 and a 3.5 MVA diesel generator as DG2 connected to bus 22 (Javadian *et al*., 2009a). The test system data are given in the Appendix.

The RBFNN for fault location has been implemented using the MATLAB software and the training data for the RBFNNs have been generated using the DIgSILENT Power Factory 14.0.516 software by simulating various types of faults created at any 100 m of each line. The target (output) vector of the RBFNNs which is the faulty line is obtained from the simulations. Table 2 summarizes the description of the inputs and outputs of the training data for the developed RBFNNs.

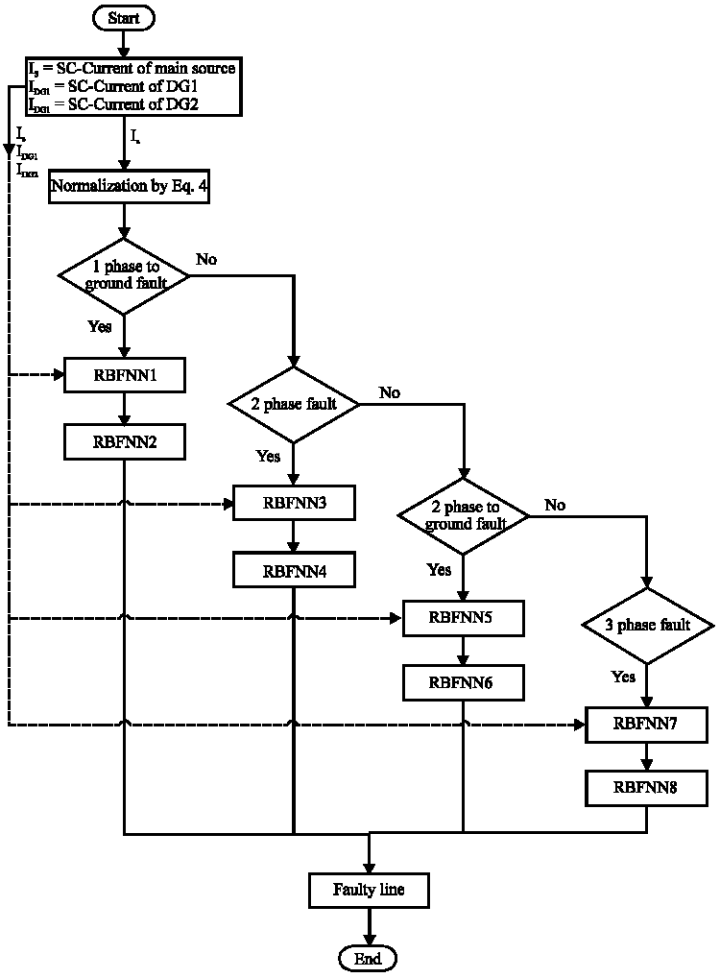

Fig. 2: Flow chart of the proposed fault location method

Table 2: Description of inputs and outputs of the RBFNN

RBFNN No.	No. of input neurons	Input description	No. of output neurons	Output description
1,3,5,7	9	3 phase short circuit current of main source and 2 DGs	3	Fault distances from the main source and 2 DGs
2,4,6,8	3	Fault distances from main source and 2 DGs	1	Faulty line

About 756 training and testing data sets have been generated with 80% of the data sets used for training the RBFNNs and 20% are used for testing to evaluate the performance of the RBFNNs. Table 3 shows the accuracy of the trained RBFNNs in which the mean square error (MSE) is less than 10×10^{-5} and the maximum training epoch is 38. During the RBFNN training, the target MSE value is set to 0.0001.

The trained RBFNNs are then tested to evaluate its performance in locating various fault types including single phase to ground fault, phase to phase fault, two phase to ground fault and three phase fault. These faults have been generated at different lengths of the distribution lines of the test system. Table 4 shows some samples of the RBFNN testing results in which RBFNN 1, 3, 5 and 7 predicts fault locations in terms of distances from the main power source and the

Table 3: Training performances of the RBFNNs

Fault type	RBFNN	MSE	Epoch
1-phase to ground	RBFNN1	5.58e-005	30
	RBFNN2	3.93e-005	35
Phase to phase	RBFNN3	7.83e-005	34
	RBFNN4	2.34e-005	38
2 phase to ground	RBFNN5	9.07e-005	29
	RBFNN6	6.58e-005	37
3 phase	RBFNN7	7.85e-005	30
	RBFNN8	4.78e-005	32

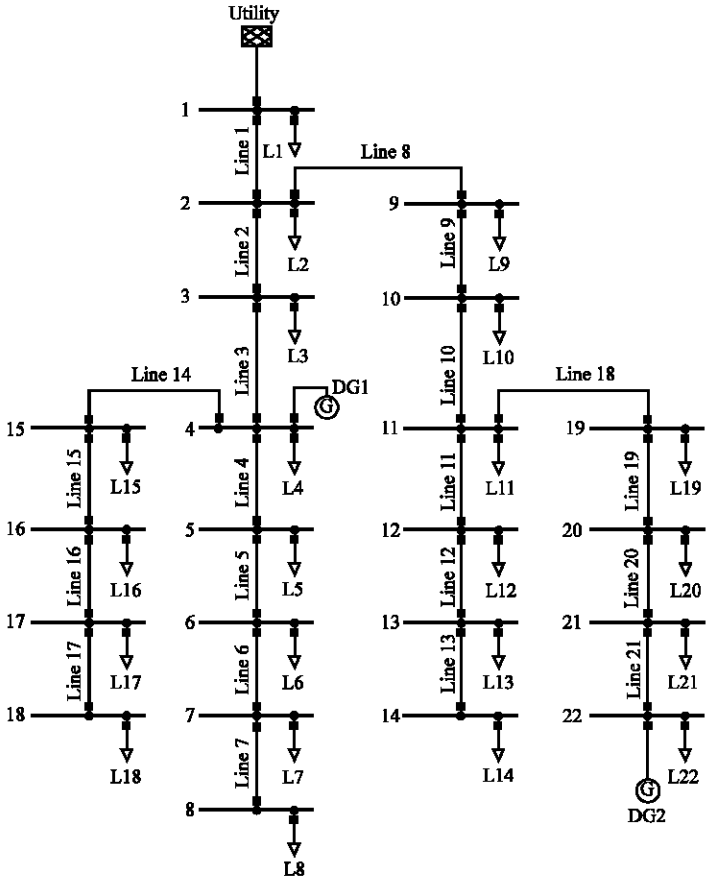

Fig. 3: Single line diagram of the test system

Table 4: Testing performance of the RBFNNs for locating faults

		RBFNN 1,3,5,7			RBFNN 2,4,6,8
Sample	Fault type	Distance from main source (km)	Distance from DG1 (km)	Distance from DG2 (km)	Faulty line No.
950 m of line 1	1-phase to ground	0.960	2.060	7.055	0.98
	Phase to phase	0.960	2.061	7.059	0.91
	2-phase to ground	0.950	2.053	7.060	1.02
	3-phase	0.961	2.057	7.057	1.07
	Actual	**0.950**	**2.050**	**7.050**	**1**
200 m of line 2	1-phase to ground	1.195	1.794	7.197	2.05
	Phase to phase	1.189	1.803	7.189	1.94
	2-phase to ground	1.211	1.802	7.193	2.03
	3-phase	1.195	1.811	7.190	2.01
	Actual	**1.200**	**1.800**	**7.200**	**2**
350 m of line 3	1-phase to ground	2.347	0.643	8.351	3.03
	Phase to phase	2.352	0.657	8.344	3.01
	2-phase to ground	2.361	0.656	8.346	3.09
	3-phase	2.355	0.647	8.351	3.05
	Actual	**2.350**	**0.650**	**8.350**	**3**
450 m of line 4	1-Phase to ground	3.450	0.453	9.442	4.01
	Phase to phase	3.449	0.458	9.449	3.98
	2-phase to ground	3.450	0.452	9.448	4.00
	3-phase	3.451	0.456	9.447	4.02
	Actual	**3.450**	**0.450**	**9.450**	**4**
560 m of line 5	1-phase to ground	4.560	1.562	10.554	4.96
	Phase to phase	4.559	1.555	10.553	4.92
	2-phase to ground	4.560	1.559	10.561	5.02
	3-phase	4.558	1.556	10.556	5.08
	Actual	**4.560**	**1.560**	**10.560**	**5**

Table 4: Continued

		RBFNN 1,3,5,7			RBFNN 2,4,6,8
Sample	Fault type	Distance from main source (km)	Distance from DG1 (km)	Distance from DG2 (km)	Faulty line No.
600 m of line 6	1-phase to ground	5.600	2.598	11.603	6.00
	Phase to phase	5.600	2.603	11.605	6.01
	2-phase to ground	5.601	2.595	11.608	6.05
	3- phase	5.602	2.601	11.604	6.04
	Actual	**5.600**	**2.600**	**11.600**	**6.00**
670 m of line 7	1-phase to ground	6.670	3.671	12.666	7.02
	Phase to phase	6.669	3.668	12.666	6.98
	2-phase to ground	6.670	3.675	12.661	7.00
	3-phase	6.668	3.671	12.666	6.97
	Actual	**6.670**	**3.670**	**12.670**	**7.00**
720 m of line 8	1-phase to ground	1.723	2.721	6.286	8.03
	Phase to phase	1.711	2.710	6.275	7.94
	2-phase to ground	1.721	2.715	6.284	8.01
	3-phase	1.718	2.719	6.281	7.98
	Actual	**1.720**	**2.720**	**6.280**	**8.00**
850 m of line 9	1-phase to ground	2.851	3.851	5.154	9.01
	Phase to phase	2.839	3.841	5.149	8.91
	2-phase to ground	2.848	3.845	5.152	8.98
	3-phase	2.842	3.843	5.145	8.93
	Actual	**2.850**	**3.850**	**5.150**	**9.00**
900 m of line 10	1-phase to ground	3.900	4.902	4.097	10.01
	Phase to phase	3.908	4.911	4.098	10.05
	2-phase to ground	3.895	4.911	4.096	9.98
	3-phase	3.907	4.908	4.101	10.03
	Actual	**3.900**	**4.900**	**4.100**	**10.00**
280 m of line 11	1-phase to ground	4.281	5.284	4.283	11.04
	Phase to phase	4.283	5.276	4.287	11.01
	2-phase to ground	4.279	5.270	4.292	10.99
	3-phase	4.284	5.273	4.289	11.02
	Actual	**4.280**	**5.280**	**4.280**	**11.00**
150 m of line 12	1-phase to ground	5.148	6.145	5.150	12.02
	Phase to phase	5.148	6.148	5.149	12.04
	2-phase to ground	5.148	6.152	5.144	12.05
	3-phase	5.146	6.153	5.144	12.01
	Actual	**5.150**	**6.150**	**5.150**	**12.00**
360 m of line 13	1-phase to ground	6.363	7.367	6.360	13.04
	Phase to phase	6.363	7.367	6.361	13.07
	2-phase to ground	6.362	7.367	6.356	13.05
	3-phase	6.363	7.365	6.362	12.93
	Actual	**6.360**	**7.360**	**6.360**	**13.00**
220 m of line 14	1-phase to ground	3.219	0.221	9.218	14.05
	Phase to phase	3.219	0.226	9.216	14.04
	2-phase to ground	3.217	0.213	9.222	14.01
	3-phase	3.219	0.228	9.210	14.03
	Actual	**3.220**	**0.220**	**9.220**	**14.00**
300 m of line 15	1-phase to ground	4.302	1.300	10.305	15.04
	Phase to phase	4.301	1.295	10.299	15.02
	2-phase to ground	4.301	1.303	10.299	15.01
	3-phase	4.299	1.296	10.301	14.98
	Actual	**4.300**	**1.300**	**10.300**	**15.00**
780 m of line 16	1-phase to ground	5.781	2.778	11.789	16.05
	Phase to phase	5.782	2.784	11.788	16.08
	2-phase to ground	5.781	2.777	11.788	16.05
	3-phase	5.783	2.782	11.787	16.09
	Actual	**5.780**	**2.780**	**11.780**	**16.00**
940 m of line 17	1-phase to ground	6.932	3.941	12.939	17.01
	Phase to phase	6.933	3.930	12.930	17.02
	2-phase to ground	6.933	3.943	12.930	17.02
	3-phase	6.931	3.936	12.931	16.98
	Actual	**6.940**	**3.940**	**12.940**	**17.00**
850 m of line 18	1-phase to ground	4.853	5.851	3.151	17.91
	Phase to phase	4.842	5.848	3.149	18.08
	2-phase to ground	4.853	5.851	3.155	18.07
	3-phase	4.854	5.859	3.147	18.06
	Actual	**4.850**	**5.850**	**3.150**	**18.00**

Table 4: Continued

		RBFNN 1,3,5,7			RBFNN 2,4,6,8
Sample	Fault type	Distance from main source (km)	Distance from DG1 (km)	Distance from DG2 (km)	Faulty line No.
420 m of line 19	1-phase to ground	5.415	6.414	2.582	19.05
	Phase to phase	5.412	6.412	2.581	18.91
	2-phase to ground	5.419	6.419	2.578	19.04
	3-phase	5.413	6.414	2.579	18.98
	Actual	**5.420**	**6.420**	**2.580**	**19.00**
250 m of line 20	1-phase to ground	6.249	7.249	1.749	20.04
	Phase to phase	6.255	7.249	1.750	20.03
	2-phase to ground	6.250	7.249	1.749	20.01
	3-phase	6.243	7.246	1.741	19.92
	Actual	**6.250**	**7.250**	**1.750**	**20.00**
570 m of line 21	1-phase to ground	7.555	8.541	0.431	21.03
	Phase to phase	7.558	8.551	0.431	20.98
	2-phase to ground	7.560	8.561	0.430	21.09
	3-phase	7.562	8.553	0.427	21.01
	Actual	**7.550**	**8.550**	**0.430**	**21.00**

two DG units while RBFNN 2, 4, 6 and 8 predicts the faulty line. Thus, the location of faults is predicted by identifying the line in the system where a fault occurs.

From Table 4, it is shown that the RBFNNs give accurate results in which the maximum error of the first RBFNN which is the difference between the actual and estimated distances of fault from the main source and all DGs is about 0.001 km. Since, each distribution line section is 1 km in length in the studied network, a deviation of 0.001 km is considered acceptable. The second RBFNN outputs after rounding to the nearest one shows the exact number of faulty lines. For instance, when a single phase to ground fault occurs at 950 m of line 1, the estimated output of the second RBFNN is 0.98 as shown on the 1st row and 4th column of Table 4. After rounding to the nearest one, the detected faulty line is line 1. The results in Table 4 also show that the second RBFNN outputs give accurate prediction of the faulty lines when compared to the actual faulty lines.

Considering more recent fault location method for a distribution network with DGs considers the application of MLPNN (Rezaei and Haghifam, 2008; Javadian *et al*., 2009a, b). Hence, to further evaluate the effectiveness of the fault location method using RBFNN, it is compared with the results of using the MLPNN. Table 5 shows the training performance of the MLPNN in which the maximum MSE value and training epoch of the MLPNN for estimating the fault distances are 0.0001 and 120, respectively. Comparing the MLPNN and RBFNN training performances, in which the maximum training epoch for RBFNN and MLPNN are 38 and 120, respectively, it can be said that the RBFNN takes shorter time to achieve the required training accuracy.

Figure 4 to 15 show the computed fault distances from each source using RBFNN and MLPNN in comparison with the actual values for single phase to ground, phase to phase, two phase to ground and three phase faults, respectively. From the figures, it is clear that the RBFNNs give outputs closer to the actual values compared to that of the MLPNN for all the fault types. Hence, the results confirm the accuracy of the RBFNN based fault location method.

Table 5: Training performances of the MLPNN

MLPNN for fault type	MSE	Epoch
1-phase to ground	2.93e-003	120
2 phase	1.08e-004	100
2 phase to ground	1.29e-003	100
3 phase	1.39e-002	110

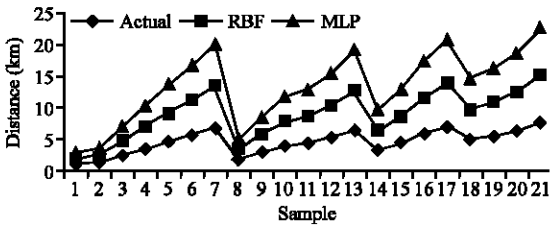

Fig. 4: The fault distance from main source for 1- phase to ground fault

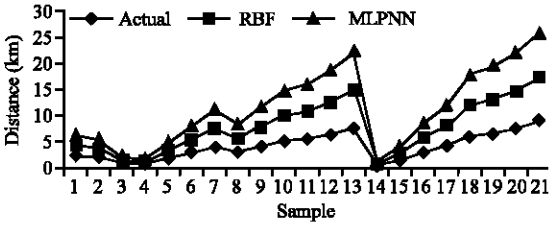

Fig. 5: The fault distance from DG1 for 1- phase to ground fault

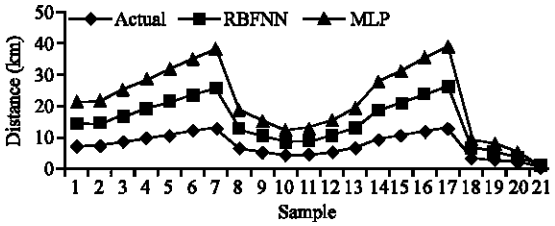

Fig. 6: The fault distance from DG2 for 1- phase to ground fault

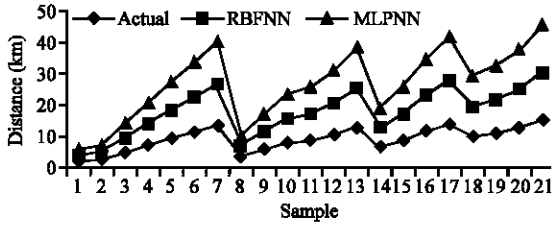

Fig. 7: The fault distance from main source for phase to phase fault

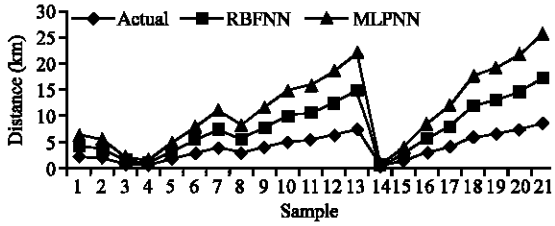

Fig. 8: The fault distance from DG1 for phase to phase fault

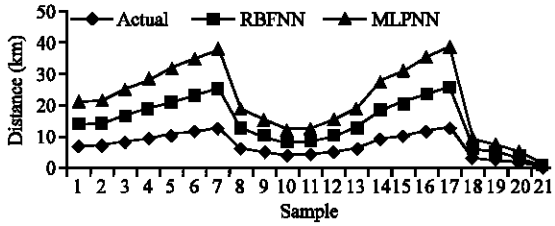

Fig. 9: The fault distance from DG2 for phase to phase fault

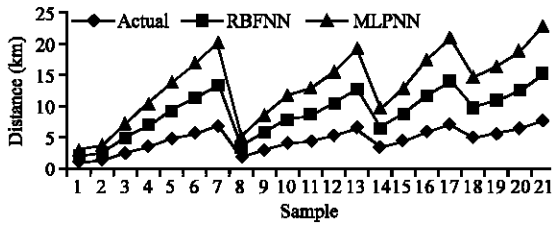

Fig. 10: The fault distance from main source for 2-phase to ground fault

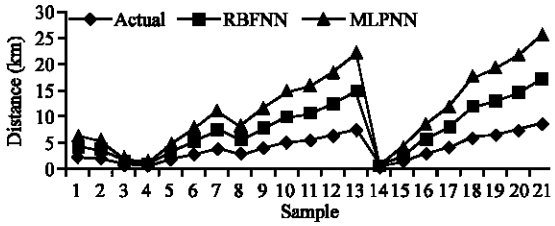

Fig. 11: The fault distance from DG1 for 2-phase to ground fault

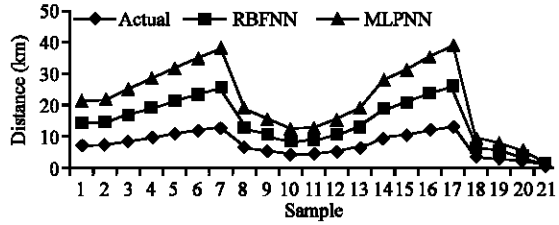

Fig. 12: The fault distance from DG1 with 2-phase to ground fault

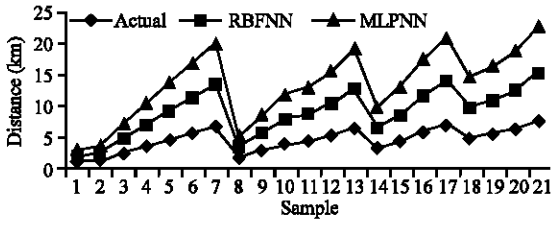

Fig. 13: The fault distance from main source for 3-phase fault

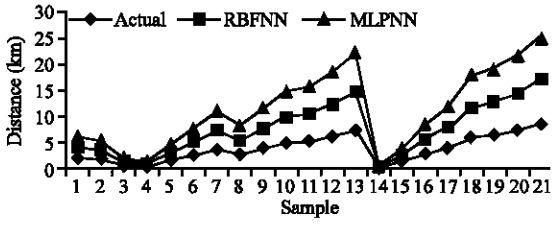

Fig. 14: The fault distance from DG1 for 3-phase fault

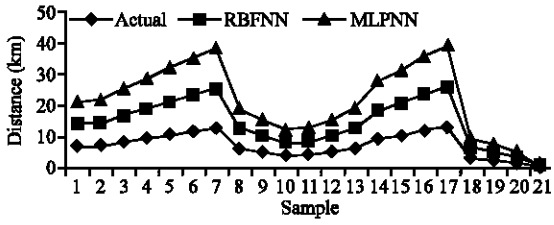

Fig. 15: The fault distance from DG2 for 3-phase fault

CONCLUSION

An automated fault location method using RBFNN for a distribution system with DG units has been presented. In the proposed approach, the normalized fault currents of the main source are used for determining the fault type and two RBFNNs have been developed for determining the fault location in a test distribution system with DGs. A test distribution system with two DG units has been selected to verify the proposed fault location method. The test results showed that the proposed RBFNN based fault location method give accurate predictions of fault distances from the main source and DG units as well the faulty lines. Furthermore, the developed RBFNNs perform better than the MLPNN in terms of accuracy and training time. The main advantage of the proposed fault location method is that it can identify the exact faulty line. Such a fault location method would be useful for assisting power engineers in performing service restoration quickly and automatically. Hence, the proposed intelligent fault location method for a system with DGs can increase network reliability; and decrease the total down time of the system.

APPENDIX

For each load a three-step hourly load curve is considered as shown in Fig. 16. The peak load for all loads is 1 MW and the power factor for all of them at each time is assumed 0.92 lagging.

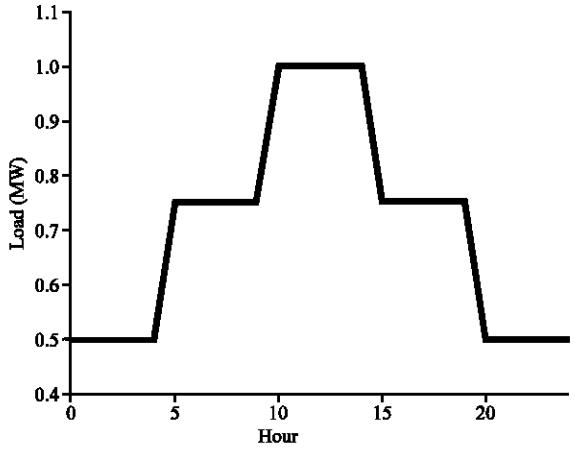

Fig. 16: Hourly load curve of the simulated feeder's loads

Table 6: Technical data of distribution lines

Conductor Name	Type	A
HYENA	ACSR	126 mm^2
Technical data	R (Ω)	0.303
	X (Ω)	0.3383
	R_0 (Ω)	0.4509
	X_0 (Ω)	1.5866
	I_n (A)	250

Table 7: Technical data of DGs

Machine type	IEC 909	Salient pole	Series 1
Voltage (kV)	20	X'd (pu)	0.256
Pn (MW)	2.8, 3.6	X"d (pu)	0.168
PFn	0.8	X0 (pu)	0.1
Connection	YN	X2 (pu)	0.2
Xd (pu)	1.5	R0=R2 (pu)	0
Xq (pu)	0.75	Rstr (pu)	0.504

All the distribution conductors are of HYENA type with 1 km length and the technical information of the conductors is given in Table 6. The technical data of all the DGs is presented in Table 7.

REFERENCES

Borghetti, A., S. Corsi, C.A. Nucci, M. Paolone, L. Peretto and R. Tinarelli, 2006. On the use of continuous-wavelet transform for fault location in distribution power systems. Int. J. Electr. Power Energy Syst., 28: 608-617.

Brahma, S.M., 2005. Fault location scheme for a multi-terminal transmission line using synchronized Voltage measurements. IEEE Trans. Power Delivery, 20: 1325-1331.

Chien, C.F., S.L. Chen and L.Y. Lin, 2002. Using Bayesian network for fault location on distribution feeder. IEEE Trans. Power Delivery, 17: 785-793.

Conti, S. and S. Nicotra, 2009. Procedures for fault location and isolation to solve protection selectivity problems in MV distribution networks with dispersed generation. Electric Power Syst. Res., 79: 57-64.

Du, J., Y. Lu, G. Zhu and X. Lin, 2009. An asymmetrical fault location method based on communication system in distribution network with DGs. Proceedings of the PSCE '09 IEEE/PES Power Systems Conference and Exposition, Mar. 15-18, Seattle,WA, pp: 1-6.

El-Fouly, T.H.M. and C. Abbey, 2009. On the compatibility of fault location approaches and distributed generation. Proceedings of the CIGRE/IEEE PES Joint Symposium on Integration of Wide-Scale Renewable Resources Into the Power Delivery System, July 29-31, Calgary, AB, pp: 1-5.

Fei, W. and S. Ying, 2003. An improved matrix algorithm for fault location in distribution network of power systems. Automation Electric Power Syst., 27: 45-46.

Gers, J. and T. Holmes, 2005. Protection of Electricity Distribution Networks. 2nd Edn., Peter Peregrinus Ltd., London.

Guo-Fang, Z. and L. Yu-Ping, 2008a. Development of fault location algorithm for distribution networks with DG. Proceedings of the IEEE International Conference on Sustainable Energy Technologies, Nov. 24-27, Singapore, pp: 164-168.

Guo-Fang, Z. and L. Yu-Ping, 2008b. A fault location algorithm for urban distribution network with DG. Proceedings of the 3rd International Conference on Electric Utility Deregulation and Restructuring and Power Technologies, April 6-9, Nanjuing, pp: 2615-2629.

Javadian, S.A.M., M.R. Haghifam and N. Rezaei, 2009a. A fault location and protection scheme for distribution systems in presence of dg using MLP neural networks. Proceedings of the PES '09 IEEE Power and Energy Society General Meeting, July 26-30, Calgary, pp: 1-8.

Javadian, S.A.M., A.M. Nasrabadi, M.R. Haghifam and J. Rezvantalab, 2009b. Determining fault's type and accurate location in distribution systems with DG using MLP neural networks. Proceedings of the International Conference on Clean Electrical Power, June 9-11, Capri, pp: 284-289.

Jun, Z., D.L. Lubkeman and A.A. Girgis, 1997. Automated fault location and diagnosis on electric power distribution feeders. IEEE Trans. Power Delivery, 12: 801-809.

Ma, J., Y. Lu, J. Du and X. Lin, 2008. A new fault location scheme based on distributed short-circuit current in distribution system with DGs. Proceedings of the IEEE International Conference on Sustainable Energy Technologies, Nov. 24-27, Singapore, pp: 1189-1194.

Mohamed, A. and M. Mazumder, 1999. A neural network approach to fault diagnosis in a distribution system. Int. J. Power Energy Syst., 19: 129-134.

Rezaei, N. and M.R. Haghifam, 2008. Protection scheme for a distribution system with distributed generation using neural networks. Int. J. Electrical Power Energy Syst., 30: 235-241.

Senger, E.C., G. Manassero, C. Goldemberg and E.L. Pellini, 2005. Automated fault location system for primary distribution networks. IEEE Trans. Power Delivery, 20: 1332-1340.

Wen, F. and C.S. Chang, 1998. A new approach to fault diagnosis in electrical distribution networks using a genetic algorithm. Artificial Intell. Eng., 12: 69-80.

Yu, L., K.K. Lai and S. Wang, 2008. Multistage RBF neural network ensemble learning for exchange rates forecasting. Neurocomputing, 71: 3295-3302.